Derivation of the tumor position from external respiratory surrogates with periodical updating of external/internal correlation.

Introduction: Techniques like beam gating or beam tracking hold promise to reduce the incidence and severity of normal tissue complications and to increase local control through dose escalation, for mobile tumors in thorax and abdomen. Precise target localization in real time is particularly important in such techniques due to the reduced clinical tumor volume to planning target volume (CTV-to-PTV) margin and/or escalated dose. Direct localization of the tumor mass in real time is difficult, if not impossible. Instead, various surrogates are used to derive the tumor position during the treatment, including implanted fiducial markers and markers placed on the surface of the patients abdomen.

The weakness of using external surrogates alone may be lack of accuracy due to the uncertainty in correlation between external surrogates and internal tumor position. The precision of tumor localization is often satisfactory with implanted fiducial markers inside or near the tumor. However, fluoroscopically tracking the markers requires radiation dose for imaging. With many treatment fractions or long treatment time of a single fraction, the imaging dose can be more than what is clinically acceptable.

In this work, we derive the tumor position from external surrogates through the calibrated external/internal correlation before each fraction of treatment. The correlation is updated during the treatment periodically by measuring the internal marker or tumor position. This way, the imaging frequency thus the imaging dose can be greatly reduced to a clinically acceptable level and the target localization accuracy can be greatly improved compared to using external surrogates alone.

Correlation function between tumor and external surrogate: The degree of correlation between the external surrogate and the tumor position was tested for eight lung patients with implanted fiducial markers at the NTT Hospital in Sapporo, Japan. Synchronized internal marker positions and external abdominal surface positions were measure during the entire course of treatment. The absolute value of the correlation coefficient computed was close to 1 in all cases, verifying a significant degree of correlation (1 is the maximum value for correlation coefficient and expresses a perfect correlation). In particular, the average absolute value of the correlation coefficient between tumor motion on the superior-inferior (SI) direction and the surrogate motion was found to be 0.95. (The range of the motion on the SI direction is the largest among the motion ranges in all three dimensions of tumor motion. For this reason and for the sake of simplicity we only focus on the SI direction of the tumor motion in the rest of the abstract).

Figure 1 illustrates the cross-correlation graph between the SI tumor motion and the surrogate motion for a particular patient.

In Figure 2 tumor positions on SI direction are scattered against the surrogate positions. The shape of the scattered values can indicate, to some extent, the characteristics of the correlation function. Changes in the slope, the offset from the origin and the width of the elliptical shapes geometrically illustrate shift, scale and phase differences among the SI tumor motion and the surrogate motion even within each breathing cycle. The correlation function should be able to count for such differences. For the purpose of this abstract a simple linear function is selected to express the observed correlation. Therefore, $\hat{y}_t = a \cdot e_t + b$, where $\hat{y}_t$ and e_t are the predicted SI tumor position and the surrogate position, respectively. The model parameter a and b express the scale and the shift difference between the external surrogate and the tumor motion, respectively.

During the patient setup session, both tumor and surrogate positions are acquired at a rate of 30Hz. Parameters a and b are estimated by fitting the linear function to the data obtained during this session (Figure 3). During treatment, tumor position is estimated based on the external surrogate position, still acquired at a 30Hz rate, and the established linear function obtained during setup session. (Figure 4).

Update methods for the correlation function: External gating implies that no tumor position is acquired during the treatment and tumor localization is based on the established during the patient setup session correlation function and the observed during treatment external surrogate positions. Under the assumption of stationary correlation, the prediction accuracy merely depends on the goodness of the function fit. However, as one can notice in Figure 4, while the predicted tumor position exhibits high accuracy during the first breathing cycle of the treatment, the accuracy declines in the succeeding breathing cycles. Further, in Figure 3, one can observe that most of the data points during treatment are located to the right of the obtained line. That indicates a dynamically varying correlation between external surrogate and tumor motion. In this case, the correlation function parameters, a and b, need to be periodically updated. Tumor images are acquired during treatment at a low frequency (e.g. 0.1Hz, i.e one image per 30 seconds) so update points (tumor versus surrogate position) can be obtained. Upon the observation of an update point,

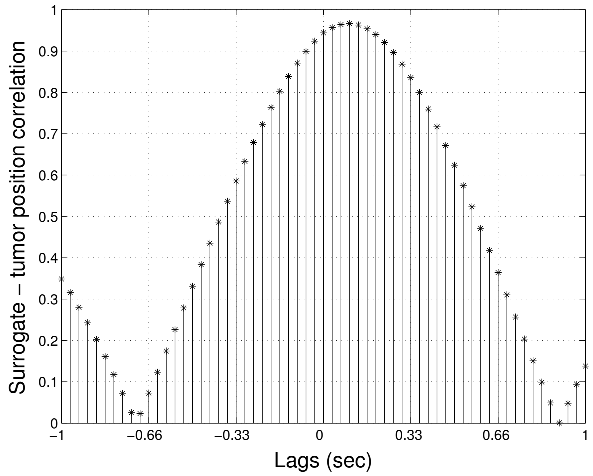

Figure 1: Cross-correlation between tumor and external surrogate motion.

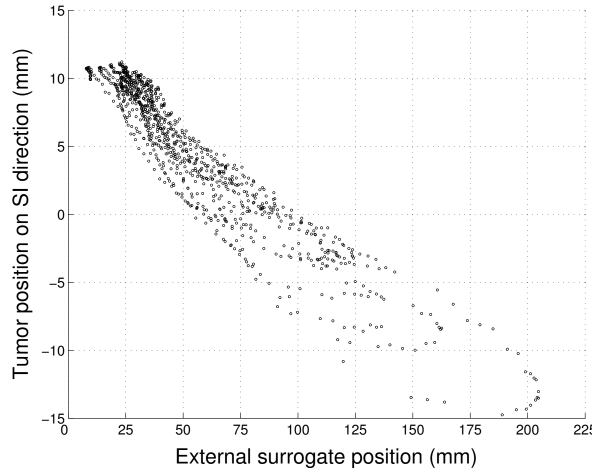

Figure 2: External surrogate position versus tumor position on the SI direction.

(e_{now}, y_{now}), different update methods to calibrate the correlation function parameters have been explored.

1. **Line Shift.** The line is shifted to pass through (e_{now}, y_{now}), i.e. b is the only parameter updated. Shift update counts only for changes in the mean position of either the tumor or the surrogate motion or both of them. For example, a patient changes position. The method aggressively corrects the correlation function, readjusting it according to the recently acquired data point.

2. **Fit model - through point.** The linear function is fitted to both training data (i.e. data gathered during the patient setup session) and data acquired during the treatment session under the constraint that passes through (e_{now}, y_{now}). The method is still aggressive but as opposed to the previous method it can compensate for both shift and scale changes in the motions relation.

3. **Fit model - extra weight.** The linear function is fitted to training data and data acquired during treatment session. Within the fitting process, (e_{now}, y_{now}) is given a larger weight than the rest of the data. In this way, previously obtained information regarding the correlation function is combined with information given by the recently acquired point. Therefore, the method moderately update the correlation function towards (e_{now}, y_{now}). Cross-validation specifies the corresponding to the recently acquired point weight.

4. **Function difference and point error.** As in the previous method does, this last method tries to balance between the need to be conservative, i.e. to keep the new model parameters close to the previous ones and corrective, thus to reduce the prediction error of new model parameters upon a future observation of (e_{now}, y_{now}).

   Let $f_{a,b}(e_t) = a \cdot e_t + b$, and $f_{a',b'}(e_t) = a' \cdot e_t + b'$, where a and b are the old function parameters while a' and b' are the ones we want to compute. Under this setup, the two extremes we could follow in order to update the model parameters would be (a) $a' = a$ and $b' = b$ (conservative) and (b) a' and b' are those parameters for which $y_{now} = a' \cdot e_{now} + b'$ (aggressive). A better idea would be to balance between the two approaches by minimizing $||f - g|| + \eta \cdot (y_{now} - a' \cdot e_{now} + b')^2$. $||f - g||$ is some distance between the two functions. In our case, $||f - g|| = (\int_{\alpha}^{\beta}((f - g)^p)$, with $e_t \in [\alpha, \beta]$. The surrogate motion range can be approximated by the motion range during the training period. If $p = 2$ then the distance above is the Euclidean (L2) distance between the two functions. The parameter η dictates how much conservative we are in our updates. Cross-validation can be used off-line to tune η.

Results of the last update method are illustrated in Figures 5 and 6. Surrogate and tumor positions during training and treatment are scattered in Figure 5. Note that the new line obtained after the update point tries to balance between the

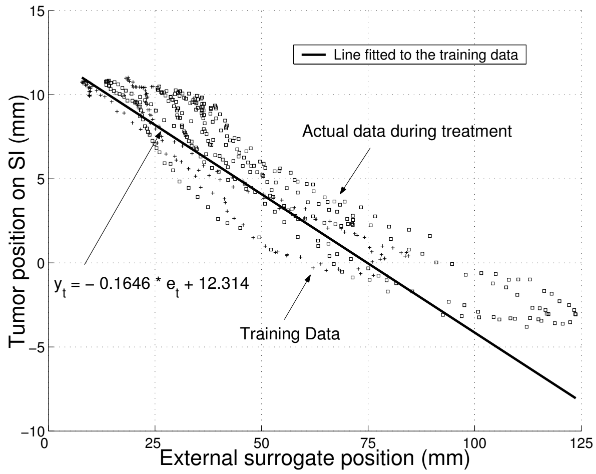

Figure 3: External surrogate position versus tumor position on SI direction during patient setup and treatment sessions. The line that best fits the training data along with the constantly obtained external surrogate positions are used to predicted the tumor position during treatment.

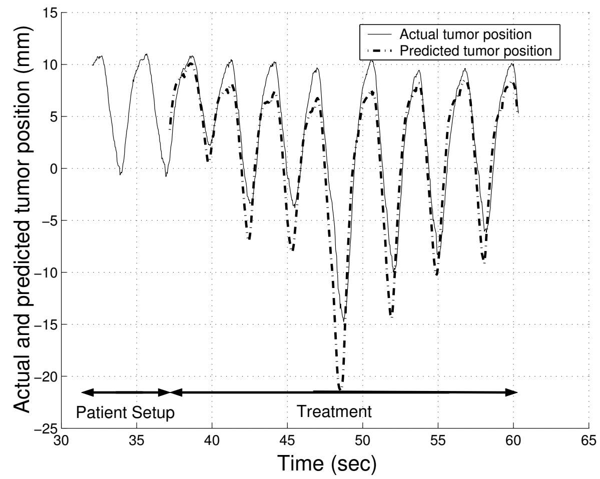

Figure 4: Actual and predicted tumor position on SI direction. After the first breathing cycle of the treatment session, there is a constant shifting between the predicted and the actual tumor position indicating a change of the correlation between tumor and surrogate motion.

line obtained during treatment and the position of the update point. Predicted and actual tumor position can be seen in Figure 6. Note the two update points and the corrected predictions after each one of them compared with Figure 4.

Results: A study has been performed first to validate that the correlation between external surrogate and tumor position is not stationary and therefore the derivation of the tumor position from external surrogates alone is inaccurate and second to compare the update methods proposed in this abstract that were used to calibrate the internal/external correlation. During the experiments, eight lung patients over several days and treatment fractions were studied. In all cases, the tumor motion from peak-to-peak varied between 8 and 41mm, with an average range of 27.69mm. The results are illustrated in Figure 7. Figure 7(b) shows the same results as (a) with a focus on frequencies less that 1Hz. In both figures the four update methods along with the no-updating case are considered and the average root mean squared (rms) error over all patients for different imaging rates ranging from 0.1 to 15Hz are plotted.

Note that for frequencies higher than 1Hz aggressive methods (*line shift* and *fit model - through point*) have lower rms error than balancing methods (*fit model - extra weight* and *function difference & point error*), while the opposite is true for frequencies lower than 1Hz. When the imaging rate is low, the number of update points obtained does not suffice to accurately characterize the changes of the correlation function. They may be outlier points. This explains the reason methods that balance their belief between previously obtained information and the update point demonstrate better results. On the contrary, when the imaging rate is high, update points can better qualify changes in correlation. In this case, larger belief on the update points results in high accuracy of predictions.

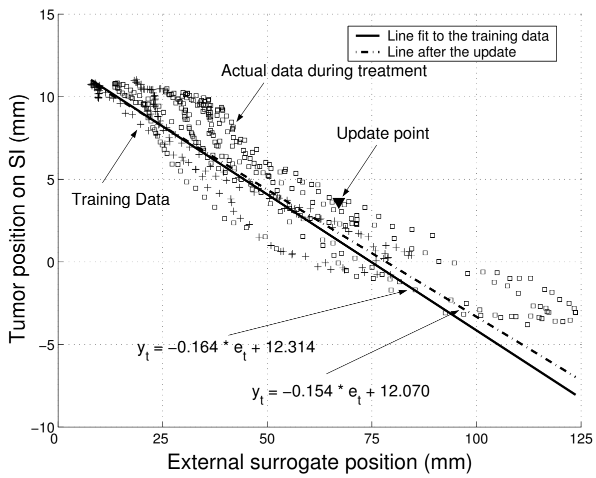

Figure 5: External surrogate position versus tumor position on SI during patient setup and treatment sessions. The line that best fits the training data along with the constantly acquired external surrogate position is used to predicted the tumor position until the tumor position is obtained (update point). An update method is used to recalibrate the line parameters.

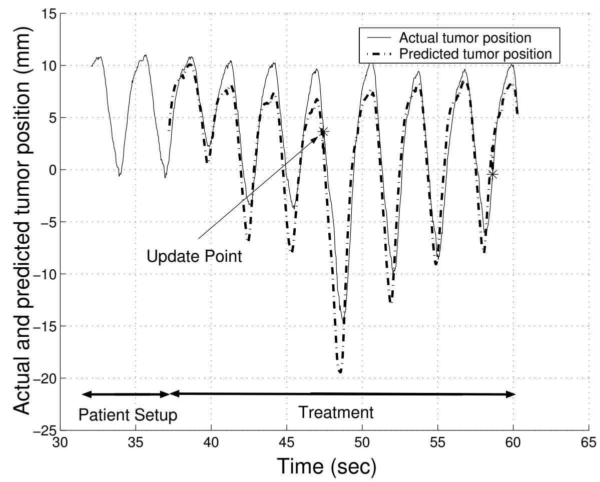

Figure 6: Actual and predicted tumor position on SI direction. Upon the observation of an update point the prediction error is partially corrected.

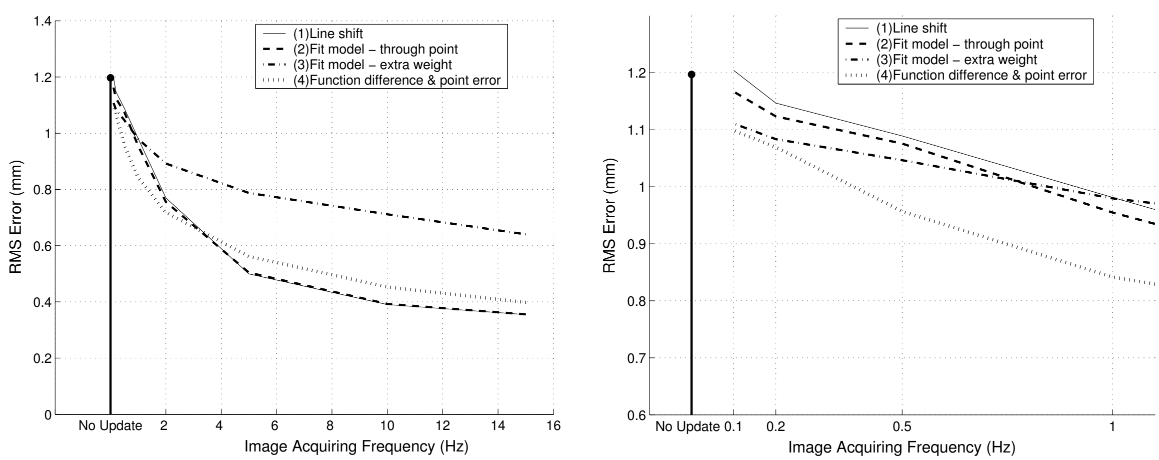

(a) (b)

Figure 7: Average RMS Error of the predicted tumor position on the SI direction considering each one of the four different update methods along with the case of no updates for different imaging rates.